Simulation of Flash-Boiling in Pressure Swirl Injectors

K. D. Neroorkar [1], S. Gopalakrishnan and D. P. Schmidt
Department of Mechanical and Industrial Engineering
University of Massachusetts - Amherst
Amherst, Massachusetts, USA 01003

R.O.Grover, Jr.
General Motors Research & Development
Warren, Michigan, USA 48090

Abstract

The use of pressure swirl injectors in wall-guided spark ignition direct-injection engines has emerged as a potential solution to decrease the specific fuel consumption of conventional port fuel injection systems. A major hurdle in the use of these injectors is that the spray characteristics, like the cone angle and drop sizes, are sensitive to the operating conditions, especially when the fuel undergoes a phase change process inside the nozzle. This phase change process, when driven by thermal effects, is known as flash-boiling. A precise control of this mechanism can be used to achieve a well atomized spray with higher cone angles and smaller drop sizes. However, such a control is extremely difficult considering the highly transient nature of the phase-change process. An accurate modeling of flash-boiling is critical if these injectors are used in practice. As this phenomenon is mainly driven by inter-phase heat transfer and has a time scale that is comparable to the flow-through times in the system, a finite rate model should be employed for these simulations. In this work, we have used the Homogeneous Relaxation Model to conduct transient, three dimensional simulations of a pressure swirl injector. The geometry includes the inlet swirl ports, the swirl chamber, the injector nozzle and the combustion chamber. A parametric study under four different operating conditions has been conducted and qualitative comparisons with experiments are presented. The working fluid used in the calculations is n-hexane and all its thermophysical properties are obtained from NIST databases.

Introduction

Recently, the automobile industry has been focusing on designing engines that can maximize fuel efficiency. The fuel economy of a diesel engine is known to be much superior to the Port-Fuel Injection (PFI) engine due to its high compression ratio and unthrottled operation. However, the diesel engine also suffers from higher noise and vibration levels, a limited speed range and higher emissions [1]. Hence research has been done to develop an engine which would exhibit a fuel economy similar to a diesel engine and, at the same time, incorporate the features of a PFI engine, like higher power output and lower emissions.

The Gasoline Direct Injection (GDI) engine promises to be a good candidate for such an engine. These engines operate on the concept of direct injection of gasoline into the combustion chamber and are known to greatly reduce the specific fuel consumption of gasoline as compared to the PFI system [1, 2]. Additionally, directly injecting gasoline into the combustion chamber provides many other critical advantages. In a PFI system, during start-up, liquid fuel collects around the intake valve area. This fuel wall wetting causes metering errors and higher emissions of unburnt hydrocarbons. The direct injection of gasoline may be able to overcome these problems since the fuel is injected directly into the cylinder. The GDI engine also offers the potential for leaner combustion, lower cylinder-to-cylinder air-fuel mixing variation, better transient response and improved air-fuel ratio control [1]. Also, due to the higher pressures in the GDI system, the fuel is much better atomized when entering the combustion chamber. However, the high velocity fuel entering the cylinder may impinge on the piston, forming a liquid film and promoting the emission of unburnt hydrocarbons. The physics of the nozzle flow is further complicated by the occurence of phase change inside the nozzle. During injection, the fuel gets heated to a high temperature by acquiring energy from the surrounding system, thereby raising its vapor pressure. Due to the high flow velocity of the fuel in the injector, the pressure falls below the vapor pressure, causing it to start vaporizing as early as the inlet corner of the nozzle. This issue

[1]Corresponding author, kneroork@engin.umass.edu

is further complicated under early injection conditions for homogeneous, warmed up, throttled operation, when the cylinder pressure may be less than the saturation pressure of the fuel. In this case, the vapor formed inside the nozzle will continue to grow and will alter the drop sizes, shape and cone angle of the resulting spray. The energy required for vaporization is provided by the liquid fuel, and this energy required increases with temperature due to a higher saturated vapor density. As a result, at higher temperatures, the time required for this inter-phase heat transfer process increases and can be comparable to the convective time scale of the flow. Under these conditions, the vaporization process is no longer an equilibrium process like cavitation, but is governed by a finite rate mechanism known as flash boiling. This process, if properly studied, can be utilized to get a higher degree of spray atomization and much better efficiency from the engine. Kim et al. [3] showed that injection of fluid with a high degree of superheat can improve engine performance due to flash boiling. Kawano et al. [4] studied the effect of flash boiling on the spray, combustion and the exhaust emissions and concluded that flashing reduced smoke emission due to better atomization

Most of the flash boiling investigations have been performed to study its effect on external sprays [5, 6, 7]. However, both Oza and Sinnamon [8] and, Park and Lee [9] noted that the phase change process begins inside the nozzle. From the experiments performed in Oza and Sinnamon [8] it is seen that that the fuel undergoes flash boiling inside the nozzle (known as the "internal flashing mode") even when the chamber pressure in the injector is above the saturation pressure of the fuel. This is attributed to the fact that the local pressure at the minimum area in the injector falls below the saturation pressure causing bubble growth and creating a two phase mixture.

Very few computational studies exist of internal flashing flows. One-dimensional models were developed and presented in Barett et al. [10] and, Chang and Lee [2], and Bianchi et al. [11] to study internal flashing flows. However these have not been tested on three dimensional simulations of complicated injector geometries. Schmidt et al. [12] presented a non-equilibrium model for flashing flows using the Homogeneous Relaxation Model (HRM). Originally applied to one-dimensional flow by Downar-Zapolski et al. [13], this model was later used in 2D simulations [14] of the flash boiling experiments of Reitz [15] and good agreement was observed with the experimental mass flow rates. Gopalakrishnan and Schmidt [16] also successfully performed a three dimensional nozzle simulation using the HRM. The current study is an extension of the work done in Gopalakrishnan and Schmidt [14, 16] to 3D simulations of pressure swirl injectors. The experimental cases of Schmitz et al. [7] are simulated and a qualitative comparison with the experimental results is presented. In addition, all fluid properties required in this work were obtained from the REFPROP database provided by the National Institute of Standards and Technology (NIST) [17].

Model Formulation

It was shown in Gopalakrishnan and Schmidt [14] that the flash boiling process takes place in thermal non-equilibrium and requires a finite rate model for the heat transfer process. There exist two alternative methods to solve this problem. The first method considers the two phases to be distinct and tracks them separately, whereas the second method uses a pseudo-fluid to represent both phases and the distinction between the phases is through the mass fraction. In our study, the pseudo-fluid approach is preferred due to its simplicity, computational efficiency and stability as compared to the former method. A limitation of our model is its inability to capture the slip velocity between the two phases; however, this assumption is much more critical in one dimensional simulations than in multidimensional dimensions [14].

The HRM, shown in Eqn. 1, is used to capture the finite rate effects of flash boiling and is based on the equation of Bilicki and Kestin [18]. In this equation, x is the instantaneous quality (mass fraction of vapor), $\overline{x}$ is the equilibrium quality, and θ is the timescale over which the x relaxes to $\overline{x}$. The time scale θ is obtained from the correlation suggested by Downar-Zapolski et al. [13] and is shown in Eqn. 2. The time scale depends on the void fraction α, and a nondimensionalized form of pressure ψ which is calculated from Eqn. 3. The variables p_{SAT} and p_C are the saturation pressure and critical pressure, respectively. The variable θ_0 is a modeling constant set to $3.84 * 10^{-7}$ seconds for all calculations presented here.

$$\frac{Dx}{Dt} = \frac{(\overline{x} - x)}{\theta} \tag{1}$$

$$\theta = \theta_0 \alpha^{-0.54} \psi^{-1.76} \tag{2}$$

$$\psi = (p_{SAT} - p)/(p_C - p_{SAT}) \tag{3}$$

The governing equations involve the continuity and momentum equations denoted by Eqns. 4 and 5, where ϕ represents the mass flux and $\overline{\overline{\tau}}$ represents the shear stress. At present, no turbulence model has been incorporated and

laminar flow is considered. The main reason for this assumption is that our main focus in this paper is understanding the effect of flash boiling on the flow. The study of flash boiling coupled with turbulence is left for future work. The molecular viscosity is obtained from the REFPROP database [17]. In addition to Eqns. 4 and 5, we solve an equation for pressure which is derived from the divergence of velocity and the HRM equation. The detailed derivation of the compressible pressure equation is presented in Gopalakrishnan and Schmidt [14]. The pressure equation is used here in its incompressible form, shown in Eqn. 6, because additional terms arising due to the compressible formulation do not appear to affect the mass flow rate solution much but slow down the rate of convergence [14].

$$\frac{\partial \rho}{\partial t} + \nabla \phi = 0 \tag{4}$$

$$\frac{\partial \rho U}{\partial t} + \nabla (\phi U) = -\nabla p + \nabla \bar{\bar{\tau}} \tag{5}$$

$$\nabla . \frac{H}{a_p} - \nabla \frac{1}{a_p} \nabla p + \frac{1}{\rho} \frac{\partial \rho}{\partial x} \mid_{p,h} \frac{Dx}{Dt} = 0 \tag{6}$$

In the above equations, concurrent with the notations of Ferziger and Peric [19], H represents the the off-diagonal components of the momentum equation and a_p denotes the diagonal term. The variable h represents the enthalpy of the fluid. An important feature of the pressure equation is that the terms containing pressure are linear and so the HRM equation can be substituted in the last term in order to close the system of equations. The system of equations were implemented in the OpenFOAM framework. [20]

Numerical Method

The continuity equation is solved implicitly, with the velocity in the mass flux term ϕ being used from the previous time iteration. The momentum and the pressure equations are solved in a coupled manner using a predictor-corrector approach similar to the PISO method [21]. In accordance with the PISO method, the pressure equation (Eqn. 6) needs to be solved iteratively to get the correct pressure field. However, the last term in Eqn. 6 introduces an added complexity due to its non-linear dependence on pressure. In order to linearize this term, a secant rule is used in conjunction with the PISO iterations. The complete details of the method employed for solving the differential equations is presented by Gopalakrishnan and Schmidt [14, 16]

Results and Discussion

The computational cases simulated here are similar to the experiments performed by Schmitz et al. [7]. Cases were simulated at temperatures of 323K, 343 K, 363 K and 381 K using n-hexane as fuel. An injection pressure of around 8 MPa and a chamber pressure of 50 KPa were used. Though all the test conditions were the same as those reported by Schmitz et al., the geometry of the injector had to be estimated since it was not reported in the paper. The high pressure swirl injector geometry used in this study was drafted using estimates of critical dimensions from Alajbegovic et al. [22] and the injector was scaled appropriately to get a fuel flow rate of 15 cm^3/s, which is consistent with the flow rate reported by Schmitz et al. The geometry and the tetrahedral grid used in the current study are shown in Fig 1. The quad-symmetry of the nozzle was utilized and simulations were done on a 90^o section of the geometry as shown in Fig 1.

An iso-contour was generated at a void fraction value of 0.8 as shown in the Fig 2(a). The average radial distance of the outer envelope of this contour was calculated at a plane which was 0.5 mm from the nozzle exit. Finally, the spray cone angle was measured as shown in the Fig.2(a). The method of fitting regression lines to the spray contours, similar to Schmitz et al., was not considered since our contours do not have as much scatter as is observed in experiments, and so a linear method is sufficient in this case. The results obtained are plotted in Fig. 2(b). It can be observed that the angle of the spray cone decreases with increasing temperatures similar to the data of Schmitz et al.[7]. In our simulations, we have observed that the exit spray cone angle is highly dependent on the internal geometry of the nozzle and so, unless the geometry used is the same, it cannot be expected that our results will exactly match the data. However, the trend of the experimental data is satisfactorily predicted, especially the sharp decrease in the angle from 323K to 343K. Since we have not included any external spray calculations, the decrease in the spray cone angle must be caused by flash boiling in the interior of the nozzle. This is similar to the “internal flashing mode” observed by Oza [23] at injection pressures above the vapor pressure of the fuel.

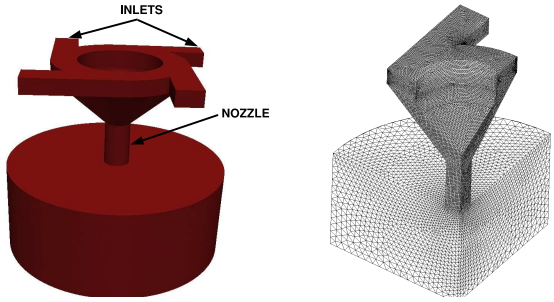

(a) Pressure-swirl injector geometry (b) Computational grid

Figure 1: Geometry and grid of the pressure swirl injector used for simulations

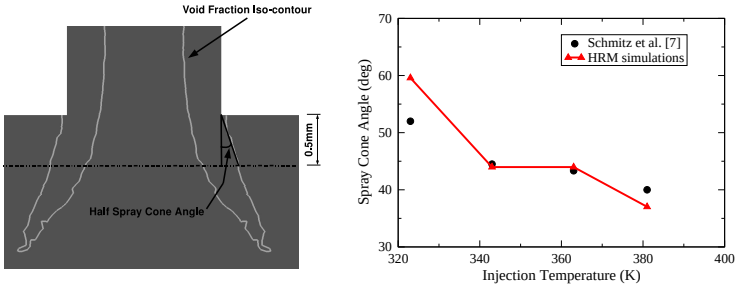

(a) Spray cone angle measurement (b) Variation of exit spray cone angle with temperature

Figure 2: Spray cone angle measurement method and results

Fig. 3 shows the contour plots of the density, void fraction, pressure and velocity for the four cases simulated, alongside the spray images from Schmitz et al. [7]. The size of the plenum chamber used in these simulations was 4 mm from the nozzle exit. Hence, the scale provided in the paper by Schmitz et al. [7] was used to extract the corresponding part of the images. It can be noted that though the velocity contour is curving towards the center with an increase in temperature, our simulations do not predict the complete collapse of the hollow cone structure which is observed in the spray images. However, in our simulations we use a single pseudo-fluid approach which assumes that the outlet chamber is filled with a mixture of fuel liquid and vapor, unlike the experiments in which air was used in the chamber. The large difference between the fuel mixture and air densities at the downstream conditions is believed to be the main reason for the cone not collapsing completely. It is also possible that, in the experiment, the cone collapses because the atomization due to flash-boiling causes smaller droplets in the spray. As these smaller droplets have lower mass, they are easily displaced by the air that is entraining from around the jet in a direction radially inwards.

Another interesting observation from the contour plots is that the region of vaporization, which usually occurs at the inlet corner of multihole injectors [16] has shifted to the center of the nozzle geometry because of the low pressure generated there from the swirling motion. At the center of the spray cone, the liquid-vapour mixture can be seen flowing from the plenum back into the swirl chamber through the center of the nozzle. The velocity of this flow increases with temperature because, as the temperature increases, the value of $psat - p$ increases, thereby reducing the time scale of vaporization according to Eqn. 2. As a result, inspite of the overall pressure gradient across the geometry remaining the same, the higher vaporization in the nozzle decreases the density of the fluid, consequently increasing its velocity.

Conclusions

The HRM was used to simulate a high pressure swirl injector using n-hexane as fuel for four different injection temperatures. Our results show a decrease in the spray cone angle as the injection temperature is increased. This trend is similar to the data of Schmitz et al. Our model also predicts the sharp decrease in the spray cone angle between injection temperatures of 323K and 343K which is attributed to the commencement of flash boiling by Schmitz et

al. Though the trend of the simulation results matches the experimental data, the exact values are different because the geometry used by Schmitz et al. was unknown to us and had to be approximated. In addition, the method used for spray cone angle measurement was different from that used by Schmitz et al. From the contour plots, it is seen that our results predict the curving of the velocity contour inwards which is believed to be a part of the cone collapse mechanism. However, the complete collapse of the spray cone, which is observed in the experiments, is not seen in the simulations. This is attributed to two possibilities: a two-phase fuel mixture was used in the exit chamber instead of air; and the simulation does not account for effects of atomization of the jet.

Acknowledgments

We acknowledge the support of General Motors and United Technologies Research Center. We further acknowledge the support of NASA under Contract No. NNC07CB05C for this work. We would also like to thank Dr. Alfred Leipertz for granting us the permission to use the spray images from the paper [7].

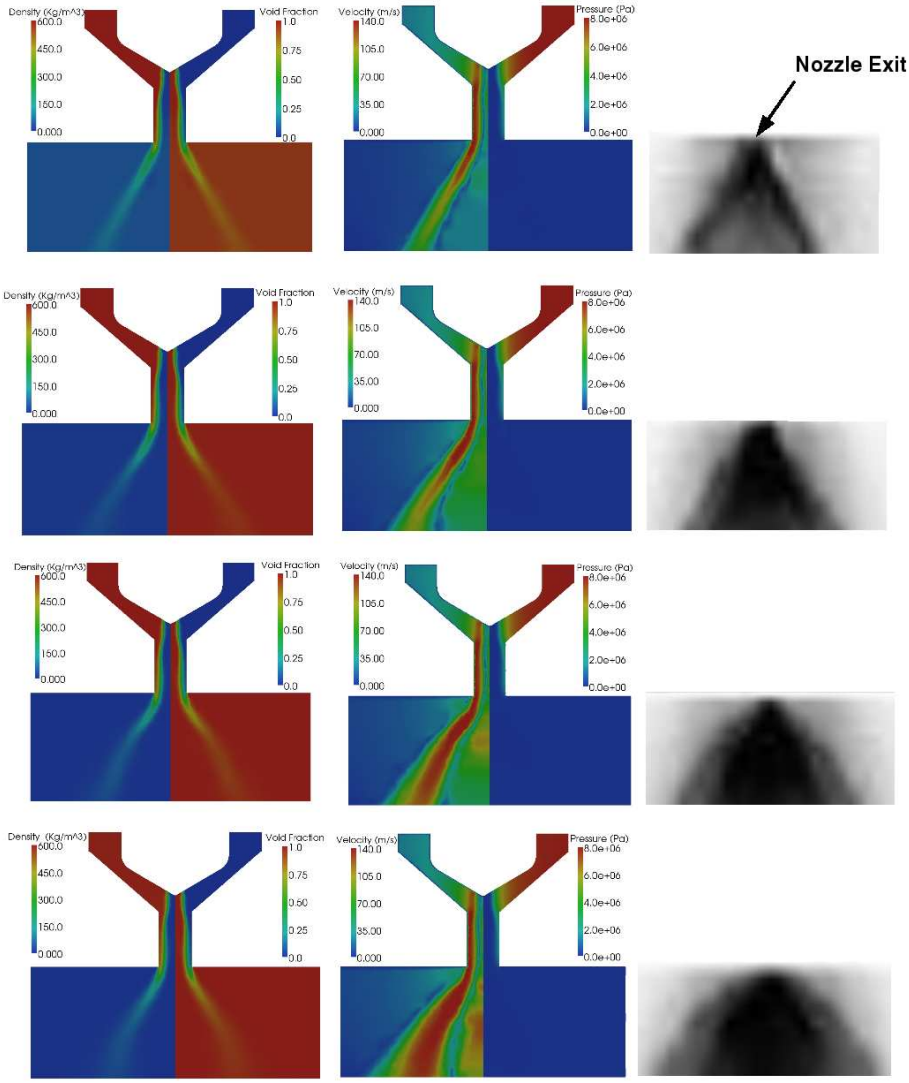

Figure 3: Computed contour plots of density, void fraction, velocity, and pressure from the present work, and experimental spray images from Schmitz et al. [7]. From top to bottom:323K, 343K, 363K and 381K.

References

[1] Zhao F., Lai M-C., and Harrington D.L. *Progress in Energy and Combustion Science*, 25:437–562, 1999.

[2] Chang D.-L. and Lee C.-F. *Proceedings of the Intersociety Energy Conversion Engineering Conference*, 37:464–469, 2002.

[3] Kim Y. K., Twai N., Suto H., and Tsuruga T. *JSAE Review*, pages 81–86, 1980.

[4] Kawano D., Senda J., Y. Wada, and Fujimoto H. *SAE paper 2003-01-1038*, 2003.

[5] Zuo B., Gomes A.M., and Rutland C. J. *International Journal of Engine Research*, 1:321–336, 2000.

[6] Acquino C., Plensdorf W., Lavoie G., and Curtis E. *SAE paper 982522*, 1998.

[7] Schmitz I., Ipp W., and Leipertz A. *SAE paper 2002-01-2661*, 2002.

[8] Oza R.D. and Sinnamon J. F. *SAE paper 830590*, 1983.

[9] Park B.S. and Lee S. Y. *Atomization and Sprays*, 4:159–179, 1994.

[10] Barett M., Faucher E., and Herard J.-M. *AIAA Journal*, 40(5), 2002.

[11] Bianchi G.M., Negro S., Forte C, Cazzoli G., and Pelloni P. *SAE paper-2009-01-1501*, 2009.

[12] Schmidt D.P., Corradini M.L., and Rutland C. J. *3rd ASME/JSME Joint Fluids Engineering Conference*, 208(616), 1999.

[13] Downar-Zapolski P., Bilicki Z., Bolle L., and Franco F. *3rd ASME/JSME Joint Fluids Engineering Conference*, 208(616), 1999.

[14] Gopalakrishnan S. and Schmidt D. P. *ILASS Americas, 21st Annual Conference on Liquid Atomization and Spray Systems, Orlando, Florida*, 2008.

[15] Reitz R. D. *Aerosol Science and Technnology*, 12:561–569, 1990.

[16] Gopalakrishnan S. and Schmidt D.P. *SAE paper-2008-01-0141*, 2008.

[17] Lemmon E.W., Huber M.L., and McLinden M.O. *NIST Standard Reference Database 23: Reference Fluid Thermodynamic and Transport Properties-REFPROP, Version 8.0*. National Institute of Standards and Technology, Gaithersburg, 2007.

[18] Bilicki Z. and Kestin J. *Proceedings of the Royal Society of London. Series A, Mathematical and Physical Sciences*, 428:379–397, 1990.

[19] Ferziger J. H. and Peric M. *Computational Methods for Fluid Dynamics*. Springer, 2002.

[20] Weller H.G., Tabor G., Jasak H., and Fureby C. *Computers in Physics*, 12(6):620–631, 1998.

[21] Issa R. I. *Journal of Computational Physics*, 62(1):40–65, 1986.

[22] Alajbegovic A., Meister G., Greif D., and Basara B. *Experimental Thermal and Fluid Science*, 26:677–681, 2002.

[23] Oza R.D. *Journal of Fluids Engineering*, 106:105–109, 1984.